

Optimization of a dynamic uncertain causality graph for fault diagnosis in nuclear power plant

Yue Zhao¹ · Francesco Di Maio² · Enrico Zio^{2,3} · Qin Zhang^{1,4} · Chun-Ling Dong⁴ · Jin-Ying Zhang⁵

Received: 4 January 2016/Revised: 11 August 2016/Accepted: 14 August 2016/Published online: 2 February 2017
© Shanghai Institute of Applied Physics, Chinese Academy of Sciences, Chinese Nuclear Society, Science Press China and Springer Science+Business Media Singapore 2017

Abstract Fault diagnostics is important for safe operation of nuclear power plants (NPPs). In recent years, data-driven approaches have been proposed and implemented to tackle the problem, e.g., neural networks, fuzzy and neuro-fuzzy approaches, support vector machine, K -nearest neighbor classifiers and inference methodologies. Among these methods, dynamic uncertain causality graph (DUCG) has been proved effective in many practical cases. However, the causal graph construction behind the DUCG is complicate and, in many cases, results redundant on the symptoms needed to correctly classify the fault. In this paper, we propose a method to simplify causal graph construction in an automatic way. The method consists in transforming the expert knowledge-based DCUG into a fuzzy decision tree (FDT) by extracting from the DUCG a fuzzy rule base that resumes the used symptoms at the basis of the FDT. Genetic algorithm (GA) is, then, used for the optimization of the FDT, by performing a wrapper search around the FDT: the set of symptoms selected during the

iterative search are taken as the best set of symptoms for the diagnosis of the faults that can occur in the system. The effectiveness of the approach is shown with respect to a DUCG model initially built to diagnose 23 faults originally using 262 symptoms of Unit-1 in the Ningde NPP of the China Guangdong Nuclear Power Corporation. The results show that the FDT, with GA-optimized symptoms and diagnosis strategy, can drive the construction of DUCG and lower the computational burden without loss of accuracy in diagnosis.

Keywords Dynamic uncertain causality graph · Fault diagnosis · Classification · Fuzzy decision tree · Genetic algorithm · Nuclear power plant

List of symbols

A	Mechanism that V induces on X
B	Failure type
CGNPC	China Guangdong Nuclear Power Corporation
DT	Decision tree
DUCG	Dynamic uncertain causality graph
F	Uncertainty relationship between variables
FD	Fault diagnosis
FDT	Fuzzy decision tree
FS	Fuzzy set
FRB	Fuzzy rule base
GA	Genetic algorithm
NPP	Nuclear power plant
r	Causal relationship intensity between each variable V and X
V	Generic variable, $V \in \{B, X\}$
X	Symptom

✉ Yue Zhao
zhaoyue0803@126.com

¹ Institute of Nuclear and New Energy Technology of Tsinghua University, Beijing 100084, China

² Energy Department, Politecnico di Milano, 20156 Milan, Italy

³ Chair System Science and the Energy Challenge, Fondation Electricité de France (EDF), CentraleSupélec, Université Paris Saclay, 92290 Chatenay-Malabry, France

⁴ Department of Computer Science and Technology, Tsinghua University, Beijing 100084, China

⁵ Department of Economic and Management, North China Electric Power University, Beijing 102206, China

Symbols

- $\boxed{N,k}$ Failure type always with $k = 1$, B type variable
- $\bigcirc_{N,k}$ Symptom, X -type variable
- \rightarrow Uncertainty relationship, F -type variable
- C Fault class
- S Symptom
- σ Observation vector
- ζ Fuzzy observation vector
- μ Element of fuzzy observation vector
- λ Classification rate
- α Number of symptoms needed for classification
- a User-defined weight for λ
- b User-defined weight for α
- Φ Objective function

Subscripts

- i Number of V , $i = 1, 2, \dots, N$
- j State of V
- k State of X
- m Number of S
- N/n Number of V

Superscript

- ' Derivative

1 Introduction

In recent years, fault diagnosis (FD) has become important for safe operation of nuclear power plants (NPPs). Fuzzy and neuro-fuzzy approaches, support vector machines [1], K -nearest neighbors [2, 3], decision tree (DT) and fuzzy decision tree (FDT) classification methods [4–9] are proposed and implemented to tackle the problem. FDT improves the DT capability by embedding fuzzy set (FS) theory in the FD and benefits of the advantages of both DT and FS. However, the not univocal correspondence between symptoms and fault classes might challenge the diagnosis task. Researches have been done in this area, and FD systems like REACTOR, SINDBAD and OAS are

developed [10–13]. All of these systems focus on the static state of NPP and method for prognostic is not mentioned. ISACS (integrated surveillance and control system) is developed in the OECD Halden Reactor Project with functions including identification of disturbance, diagnosis and prognostics [14–16]. This system mainly contains two parts: prior diagnosis, which is model-based; and on-line diagnosis, which is based on comparing the fault data with those in Process and Automatics (P&A) data base. Unfortunately, the prototype ISACS-1 is mainly utilized for extensive evaluation and further progression of the system has not been elaborated. In other FD systems, some are based on the complete model of the industrial systems [17–21], which is difficult to be applied on the systems whose complete model are hard to build. While some other systems are data mining based [19, 22], which is difficult for NPPs because it is often difficult to obtain fault data to train the classification model. J. Ma and J. Jiang developed a FD system based on semisupervised classification scheme, which was considered as a promising tool [23]. However, the model are trained by the data of normal power plant, which may not diagnose the faults that owned only by NPPs.

Recent works on classic uncertain artificial intelligence methodology, such as rough set [24, 25], artificial neural network (ANN) [26, 27], fuzzy theory [28–30], gray relational analysis [31, 32], petri nets [33, 34] and support vector machine (SVM) [35, 36], are introduced and combined for FD and prognostic in complex systems. Also, probabilistic graphical model has become new hotspot in this field, and the Bayesian networks (BN) model [37, 38], Hidden Markov Models (HMM) [39–41], latent tree models (LTM) [42] and cloud models [43] draw high attention. BN is especially typical. It is of solid theoretical foundation, with directed acyclic graph to express causal dependency and conditional probability table to quantify the uncertainty of causality. To improve the efficiency of FD, a graphical inference methodology named Dynamic Uncertain Causality Graph (DUCG) has been developed and successfully tested in many practical cases [44–51].

DUCG implements a causal-based expert system that represents the knowledge of risk experts in either a directed

Table 1 Variables (events) in DUCG (N , the variable number; k , state)

Variable	Symbol	Meaning
B	$\boxed{N,k}$	Failure type always with $k = 1$
X	$\bigcirc_{N,k}$	Symptom
$F_{n,k;i,j}$	\rightarrow	Uncertainty relationship between variable $V_{i,j}$ in state j ($V \in \{B, X\}$, $i = 1, 2, \dots, N$) and variable $X_{n,k}$ in state k , where $i \neq n$ and $j \neq k$

Fig. 1 Examples of weighted functional elements (a) and a simple DUCG (b)

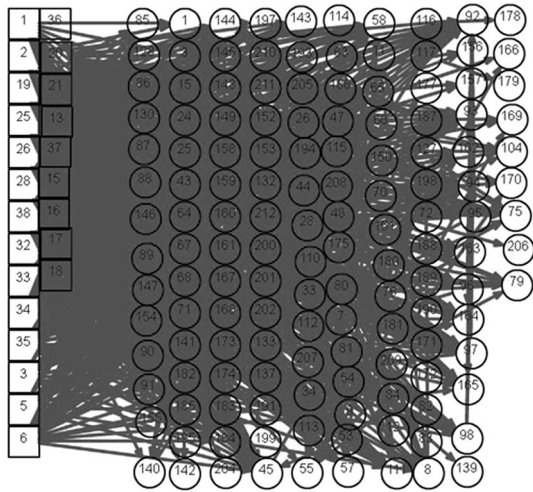
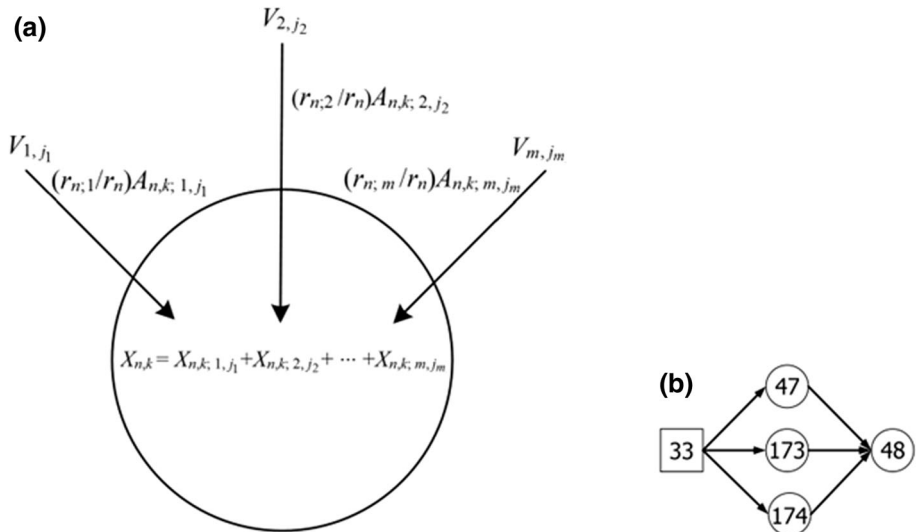


Fig. 2 DUCG of the secondary loop of Unit-1 of Ningde NPP

acyclic graph or a directed cyclic graph, with a probabilistic-based or evidence-based reasoning [44, 45]. Nevertheless, the causal graphs construction of DUCG is complicate in some cases, turning out redundant on the symptoms needed by DUCG to correctly classify the occurring faults [46–51]. In this paper, we propose a method to simplify the inference rules of DUCG based on a genetic algorithm (GA) that uses an FDT as surrogate model of the DUCG.

This paper is organized as follows. In Sect. 2, a brief introduction to the DUCG is given, including the inference algorithm used for fault diagnosis and the steps required for constructing the DUCG model. Section 3 illustrates the method for transforming the expert knowledge into a FDT by extracting a fuzzy rule base (FRB) from a first-tentative DUCG model that provides a non-optimal symptom matrix. In Sect. 4, GA is used for the optimization of the

decision rules by performing a wrapper search around the FDT and results are discussed. In Sect. 5, conclusions are drawn.

2 Brief introduction to DUCG

The methodology of DUCG is essential to apply the causal graphs to symbolize logical relationships in complex system in reality and to apply the virtual variables to express the causal uncertainties in that relationships, that is, the probabilities between child and parent variables. DUCG provides a compact representation of the existing causal logic among events that can occur in a process [45, 46], by resorting to causal graphs composed by variables (or events) (as illustrated in Table 1, where “V” is a generic variable and “N” and “k” are the variable number and state, respectively), connected by function F .

We can define $F_{n;i}$ as a graph composed of elements connected by $F_{n,k;i,j}$ [45], as shown in Fig. 1a, that can be defined as:

$$F_{n,k;i,j} = (r_{n;i}/r_n)A_{n,k;i,j}, \tag{1}$$

where $A_{n,k;i,j}$ accounts for the mechanism that $V_{i,j}$ induces on $X_{n,k}$, without considering any other natural interaction with other mutual variables $B_{i,j}$, $j' \neq j$; and $(r_{n;i}/r_n)$ is a weighting factor of $A_{n,k;i,j}$, with $r_n \equiv \sum_i r_{n;i}$ and $r_{n;i}$ being the causal relationship intensity between each V_i and X_n [45–48].

The procedures for building a DUCG can be summarized as follows:

1. A detailed analysis of the system to identify all B type variables (i.e., fault types);

Table 2 The 23 fault classes (variables of type B)

No.	Root cause	Description
1	$B_{1,1}$	Condensate pump CEX001PO fails open
2	$B_{2,1}$	Condensate pump CEX002PO fails open
3	$B_{3,1}$	Feedwater control valve ARE031VL stuck open
4	$B_{5,1}$	Feedwater control valve ARE032VL stuck open
5	$B_{6,1}$	Feedwater control valve ARE033VL stuck open
6	$B_{20,1}$	Leakage in the feedwater pipeline B
7	$B_{21,1}$	Leakage in the feedwater pipeline C
8	$B_{13,1}$	Turbine mechanical failure with no reactor trip
9	$B_{37,1}$	Loss of main steam in turbine
10	$B_{15,1}$	Leakage in the low pressure heater ABP401RE
11	$B_{16,1}$	Feedwater heater bypass valve ABP011VL stuck open
12	$B_{17,1}$	Leakage in the main steam pipeline
13	$B_{18,1}$	Leakage in the steam generator pipe
14	$B_{19,1}$	Feedwater heater AHP009VL stuck open
15	$B_{25,1}$	Electric main feedwater pump APA102PO fails
16	$B_{26,1}$	Electric main feedwater valve APA113VL stuck close
17	$B_{38,1}$	Steam generator loss of feedwater
18	$B_{28,1}$	Condensate extraction valve CEX108VL stuck open
19	$B_{32,1}$	Turbine bypass valve GCT115VV stuck open
20	$B_{33,1}$	Leakage in the steam line A
21	$B_{34,1}$	Turbine bypass valve GCT131VV stuck open
22	$B_{35,1}$	Turbine control valve GRE001VV stuck open
23	$B_{36,1}$	Condenser vacuum pump CVI101PO stuck open

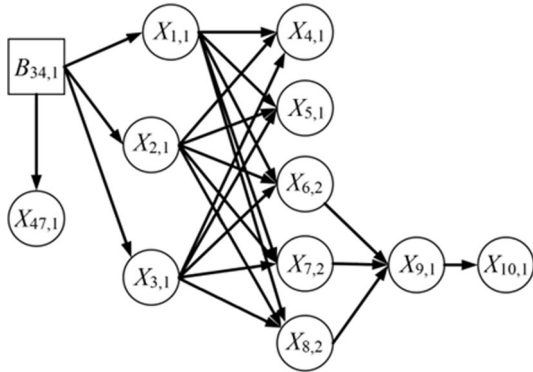


Fig. 3 One fault in DUCG model

- To determine the related X -type variables for each of the B type variables;
- To quantify the causal relationships, i.e., the F -type variables.

For example, in Fig. 1b, $B_{33,1}$ indicates the leakage in the steam pipeline A, variable X_{47} , X_{173} and X_{174} represent the steam flow in pipelines A/B/C of a NPP, respectively; and X_{48} indicates the pressure in the steam pipeline A, where the normal, low and high pressure states are $X_{48,0}$, $X_{48,1}$ and $X_{48,2}$, respectively. The relationship, for example, between X_{48} and X_{47} can be modeled by $F_{48;47} = (r_{48;47}/$

$\sum r_{48;i}) A_{48;47}$, where $\sum r_{48;i} = r_{48;47} + r_{48;173} + r_{48;174}$ (with $r_{48;47} = r_{48;173} = r_{48;174} = 1$) and $A_{48;47}$ (the uncertain mechanism that links the three states of X_{47} to the three states of X_{48}) is

$$A_{48;47} = \begin{pmatrix} 0 & 0 & 0 \\ 0 & 0.1 & 0.7 \\ 0 & 0.9 & 0.3 \end{pmatrix},$$

which means that when X_{47} is in its “1” state $X_{47,1}$, the probabilities of the X_{48} in the “0” state $X_{48,0}$ is 0, in the “1” state $X_{48,1}$ is 0.1 and in the “2” state $X_{48,2}$ is 0.9. Similarly, when X_{47} is in its “2” state $X_{47,2}$, the probabilities of the $X_{48,0}$, $X_{48,1}$ and $X_{48,2}$ are 0, 0.7 and 0.3, respectively.

By utilizing this modeling method, the DUCG of the secondary loop of Unit-1 of Ningde NPP is shown in Fig. 2. The causal graph is of great complexity, including 151{ B,X } type variables and 976 functional relationships, of which 23 variables of type B (fault classes) are given in Table 2.

After construction of the DUCG model based on the expert knowledge regarding the expected progression of an accidental scenario, that allows setting the functional relationship among the variables, the diagnosis can be carried out by monitoring the signals behavior during the developing accidental scenario.

Table 3 Symptom matrix

C1	1	1	0	0	0	0	0	0	0	0
C2	1	1	0	0	0	0	0	0	0	0
C3	0	0	0	0	0	0	0	0	0	0
C4	0	0	0	0	0	0	0	0	0	0
C5	0	0	0	0	0	0	0	0	0	0
C6	0	0	0	1	0	0	0	0	1	1
C7	0	0	0	1	0	0	0	0	1	1
C8	0	0	0	0	0	0	0	0	0	0
C9	0	0	0	0	0	0	0	0	0	0
C10	0	0	0	0	1	0	1	0	0	0
C11	0	0	0	0	0	1	0	0	0	0
C12	0	0	0	0	0	0	1	0	0	0
C13	0	0	0	0	0	0	0	0	0	0
C14	0	0	0	0	1	0	0	1	0	0
C15	0	0	1	0	1	0	0	1	1	1
C16	0	0	1	1	0	1	0	1	0	0
C17	0	1	0	0	0	1	1	0	0	0
C18	0	0	0	0	0	0	0	0	0	0
C19	0	0	0	0	0	0	0	0	0	0
C20	0	0	0	0	0	0	0	0	0	0
C21	0	0	0	0	0	0	0	0	0	0
C22	0	0	1	0	0	0	0	0	0	0
C23	0	0	0	0	0	0	0	0	0	0
C1	0	0	0	0	0	0	0	0	0	0
C2	0	0	0	0	0	0	0	0	0	0
C3	0	0	1	1	0	1	0	0	0	0
C4	0	0	0	0	0	0	0	0	0	0
C5	0	0	1	0	0	0	0	0	0	0
C6	1	0	0	1	0	0	0	0	0	1
C7	1	0	0	0	0	0	0	0	0	1
C8	0	0	0	0	0	1	0	0	0	0
C9	0	0	0	0	0	1	0	0	0	0
C10	0	0	0	0	0	0	0	0	0	0
C11	0	0	0	0	0	0	0	0	0	0
C12	0	1	1	0	0	0	0	0	0	1
C13	0	0	0	0	0	0	0	0	0	0
C14	0	1	0	0	0	0	0	0	0	0
C15	1	0	0	0	0	0	1	1	1	0
C16	0	1	0	1	1	0	1	1	1	1
C17	0	0	0	0	1	0	0	0	0	0
C18	0	0	0	0	0	0	0	0	0	0
C19	0	0	0	0	0	0	0	0	0	0
C20	0	0	0	0	0	0	0	0	0	0
C21	0	0	0	0	0	0	0	0	0	0
C22	0	0	0	0	1	0	1	1	1	0
C23	0	0	0	0	0	0	0	0	0	0

For better illustration, let us focus on the types and states of the variables shown in Fig. 3. The fault $B_{34,1}$ can be diagnosed as “turbine bypass valve GCT131VV wrongly opened during NPP normal operation” because it initiates the flow decrease in Steam pipelines A, B and C ($X_{1,1}, X_{2,1}, X_{3,1}$), which, subsequently, decreases the pressure in the steam manifolds VVP024MP and VVP025MP ($X_{4,1}, X_{5,1}$), and increases the feedwater flow in the stream generators SG-1, SG-2 and SG-3 ($X_{6,2}, X_{7,2}, X_{8,2}$). The reduction of the feedwater flow can further induce the average temperature to decrease in the first loop ($X_{9,1}$) and, eventually, cause the increase of the reactor power ($X_{10,1}$).

Therefore, a specific state of a B -type variable corresponds to a set of X -type variables, which are all abnormal signals received from the sensor measurements. In other words, when a generic fault of class $C_j, j = 1, 2, \dots$ occurs, a set of representative symptoms emerge that might not be univocal, as in this case.

3 From DUCG to fuzzy decision tree

The FDT methodology is selected to speed up the optimization of the DUCG model in the case of non-univocal symptoms. The FDT is used as surrogate model of the DUCG, whose fuzzy rules are to be extracted from the DUCG model to build the FRB knowledge. A first-tentative prior FRB is chosen to represent the classification reasoning. The FRB is composed of several fuzzy rules, each one related to a specific FS for each fault class $B_{i,j}$. As an example, with reference to Fig. 3, the fuzzy rule defining $B_{34,1}$ can be written as: “IF the flow in steam pipeline A, B and C is low ($X_{1,1}, X_{2,1}, X_{3,1}$); the pressure in steam manifolds VVP024MP and VVP025MP is low ($X_{4,1}, X_{5,1}$); the feedwater flow in stream generators SG-1, SG-2 and SG-3 is high ($X_{6,2}, X_{7,2}, X_{8,2}$); the average temperature in the first loop is low ($X_{9,1}$) and the reactor power is high ($X_{10,1}$), THEN the turbine bypass valve GCT131VV has been wrongly opened ($B_{1,1}$)”. Symptoms of X -type variables mentioned in the fuzzy rule can be summarized into an observation vector $\sigma = (X_{1,1}, X_{2,1}, X_{3,1}, X_{4,1}, X_{5,1}, X_{6,2}, X_{7,2}, X_{8,2}, X_{9,1}, X_{10,1})$. All the fuzzy rules defining the relationships between symptoms and the 23 fault classes can be resumed in the symptom matrix (shown in Table 3 in a reduced form), in which the rows and columns are fault classes and symptoms, respectively, where “1” means that the symptom can be observed for the fault considered, and “0”, otherwise. We note that the relationship between symptoms and fault classes is not univocal, that is, one

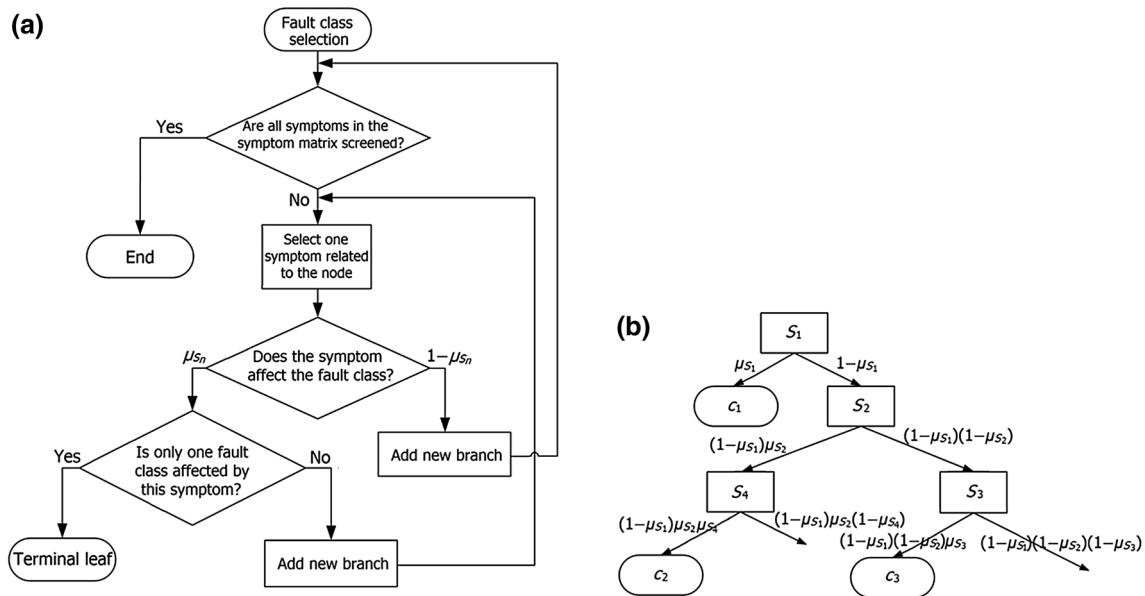


Fig. 4 Steps for building a FDT (a) and example of a FRB-FDT (b)

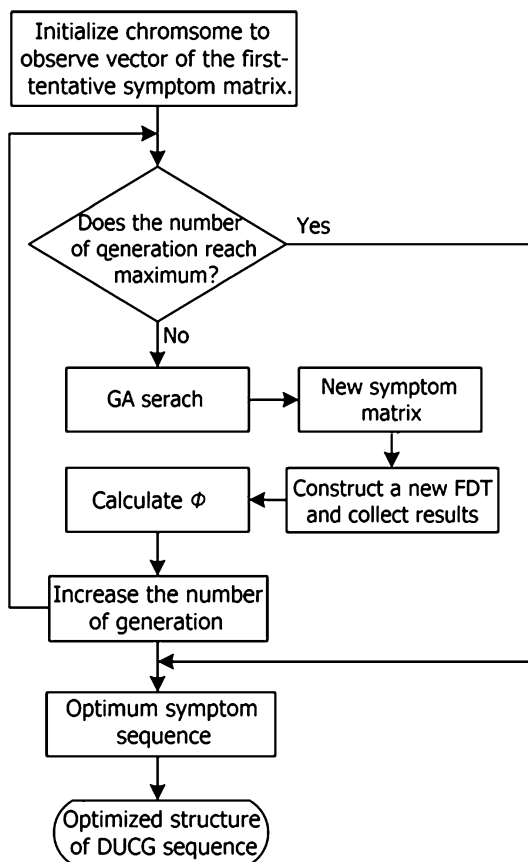


Fig. 5 Wrapper research with GA

symptom may lead several faults and one fault can be inferred only when several symptoms are simultaneously observed. This is mainly due to the complex nonlinear

Table 4 GA main parameters

Objective function	$\Phi = a(1 - \lambda) + bx$
Number of chromosomes in the population	270
Number of generations	100
Selection	Standard Roulette
Replacement	Children-Parents
Mutation probability	0.001
One-site crossover probability	1

relationship of the events, but also to the partial and sometimes overwhelming expert knowledge at the basis of the DUCG.

Sensor errors and ambiguous deviation ranges (that is, uncertainty in the symptoms values) can be accommodated in the FRB by defining a fuzzy observation vector $\varsigma = (\mu_{S_1}, \mu_{S_2}, \dots, \mu_{S_n})$, in which each element μ_{S_n} is the degree of membership of a symptom S_n to the FS “symptom occurrence”.

The construction of the FDT aimed at substituting the DUCG within the GA-based optimization of the FRs can be done as shown in Fig. 4a; in particular:

1. Choose one fault class of the DUCG;
2. Select one symptom S_n ;
3. Branch the tree based on presence or absence of the symptom for the fault class considered by accounting for its membership degree μ_{S_n} ;
4. If the symptom can be attributed to only one fault class, the associated node becomes a terminal leaf, otherwise, a new node is added with membership degree $(1 - \mu_{S_n})$ and procedure starts again from 2.

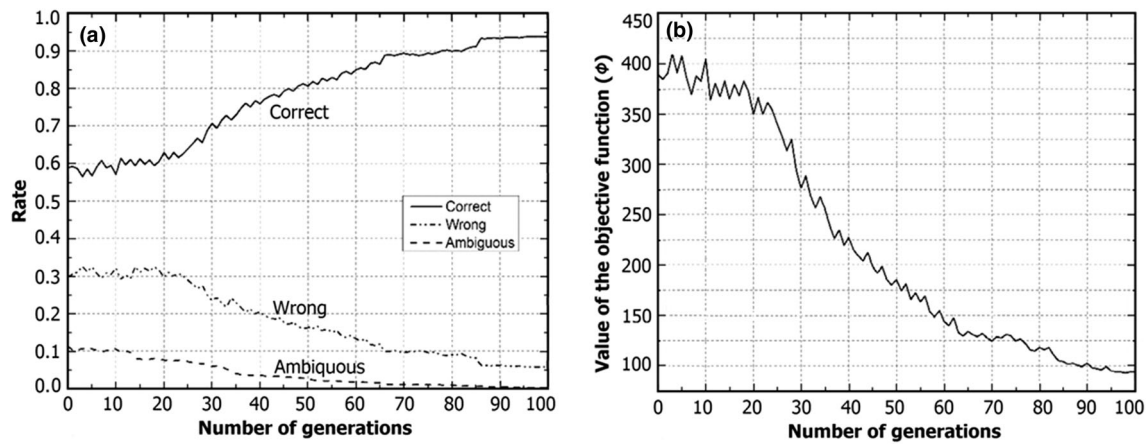


Fig. 6 Results of optimization

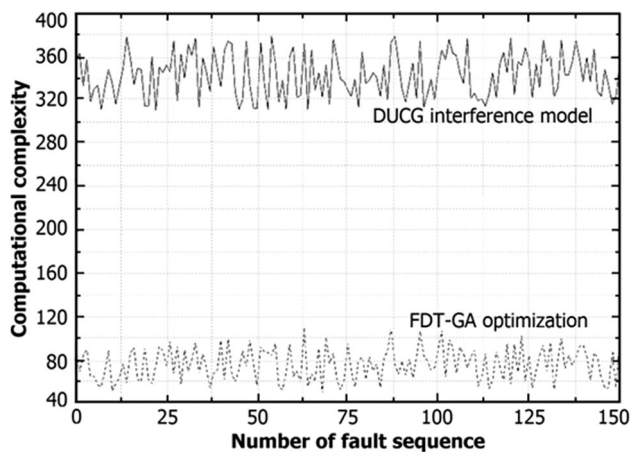


Fig. 7 Results in computation complexity

When all symptoms are screened out and placed in related branches, the tree is terminated. Figure 4b shows a general example of a FRB-FDT.

With the method illustrated above, the symptom matrix of Table 3 of the DUCG model in Fig. 2b is learnt by a FRB-FDT with 23 fault classes and 262 symptoms. The developed FRB-FDT is tested with respect to 800 data synthetically simulated by the China Nuclear Power Simulation Technology Co, Ltd. (CNPSC). The results indicate that 58.9% of the anomalous behaviors are correctly classified with respect to the 23 classes, 29.7% are treated as ambiguous and 11.4% are wrongly classified due to the ambiguous assignment between symptoms and fault classes of the initial structure of DUCG based FRB-FDT (for the classification rate quantification, we assume the assignment to be correct when the membership grade to a class is greater than 0.8, ambiguous when is between 0.8 and 0.2 and wrong when it is lower than 0.2).

4 GA optimization of the inference rules

To improve the classification rate of the DUCG and lower its computational burden, thanks to a simpler symptoms-fault relationship, a single-objective GA-based optimization is conducted for finding the most representative symptom matrix that would best describe the system behavior. We resort to the wrapper search scheme shown schematically in Fig. 5.

A symptoms observation vector σ becomes a chromosome of the GA, and the fitness function to evaluate the performance of a set of symptoms in classifying the faults is defined as:

$$\Phi = a(1 - \lambda) + b\alpha, \tag{2}$$

where $a(1 - \lambda)$ accounts for the classification rate λ of the FDT, and $b\alpha$ accounts for the number α of symptoms needed for classifying as many as possible fault classes, since the optimization must obey a parsimony principle (i.e., low α is preferable) to guarantee a low computational complexity of DUCG and a large classification rate, i.e., low $(1 - \lambda)$. The objective (fitness) Φ must be minimized. The parameters a and b are user-defined weight, and here we set $a = 80$ and $b = 1$, so as to balance the different magnitudes of $(1 - \lambda)$ and α , and normalize their mutual contribution to Φ . The main parameters of the GA used are listed in Table 4.

GA can better select symptoms for each fault class, hence the improvement of performance. The results of optimization are shown in Fig. 6. In Fig. 6a, the rate of correct classification increases with the number of generations, while the rates of ambiguous and wrong classifications decrease. The three rates reach steadiness at the 90th generation, being 93.8, 5.9 and 0.4%, respectively. In Fig. 6b, the value of objective function decreases with increasing number of generations. This indicates that the new set of selected chromosomes can neglect the

contradictory assignments between symptoms and fault classes, but, rather, link them without ambiguity. Therefore, the GA optimization of the symptom matrix is beneficial to the FDT and, thus, to the DUCG that would be built on the basis of these results.

To be more accurate, one experiment based on 150 fault sequences is carried out to verify the reduction in computation complexity. Figure 7 shows the results by initial DUCG inference model and the 100th generation of FDT-based GA optimization. The number of symptoms needed for classification of maximum fault classes, that is, α in Eq. (2), is used to measure the computation complexity. It is shown that the computational complexity can be significantly reduced after the optimization and the degrees of computation reduction are all above 70.5%, maximum to 84.95%.

5 Conclusion

DUCG is an interesting method for fault diagnosis for industrial systems. However, causal graphs that are built by DUCG for inferring the fault classes can become huge for complex systems (as for the example of the secondary loop in Unit-1 of Ningde NPP here considered). This also leads to a computational burden when performing the diagnosis.

To optimize the DUCG model, we have proposed to substitute it with a FDT and to optimize the symptom matrix of this FRB model by a single-objective GA. A wrapper search is carried out to look for the set of observations (coded into GA chromosomes) that best characterize the failure behavior of the system. This is expected to lead to twofold benefits: improvement of the classification rate and decrease of the complexity of the DUCG model.

Experimental results on a set data from a simulator of the secondary loop in Unit-1 of Ningde NPP demonstrate that the application of GA for optimizing a FDT-based DUCG is effective in optimizing the DUCG model.

However, some unique properties of DUCG, such as the effect of combination of several symptoms to a fault, the hidden relationships among different symptoms and the process of time sequence in some cases are not considered in this paper, which our future work focused on.

References

1. J.A.K. Suykens, J. Vandewalle, Least squares support vector machine classifiers. *Neural Process. Lett.* **9**(3), 293–300 (1999). doi:[10.1023/A:1018628609742](https://doi.org/10.1023/A:1018628609742)
2. B. Kosko, *Neural Networks and Fuzzy Systems: A Dynamical Systems Approach to Machine Intelligence/Book and Disk*, vol. 1 (Prentice Hall, Englewood Cliffs, 1992). doi:[10.1017/S0269888900008225](https://doi.org/10.1017/S0269888900008225)
3. P.M. Frank, Fault diagnosis in dynamic systems using analytical and knowledge-based redundancy: a survey and some new results. *Automatica* **26**(3), 459–474 (1990). doi:[10.1016/0005-1098\(90\)90018-D](https://doi.org/10.1016/0005-1098(90)90018-D)
4. E. Zio, P. Baraldi, I.C. Popescu, From fuzzy clustering to a fuzzy rule-based fault classification model. *Int. J. Comput. Intell. Syst.* **1**(1), 60–76 (2008). doi:[10.1080/18756891.2008.9727605](https://doi.org/10.1080/18756891.2008.9727605)
5. E. Zio, P. Baraldi, I.C. Popescu, A fuzzy decision tree for fault classification. *Risk Anal.* **28**(1), 49–67 (2008). doi:[10.1111/j.1539-6924.2008.01002.x](https://doi.org/10.1111/j.1539-6924.2008.01002.x)
6. P. Baraldi, F. Di Maio, E. Zio, Unsupervised clustering for fault diagnosis in nuclear power plant components. *Int. J. Comput. Intell. Syst.* **6**(4), 764–777 (2013). doi:[10.1080/18756891.2013.804145](https://doi.org/10.1080/18756891.2013.804145)
7. E. Zio, F. Di Maio, Fuzzy similarity-based method for failure detection and recovery time estimation. *Int. J. Perform. Eng.* **6**(5), 407–424 (2010). http://www.researchgate.net/publication/282063966_A_fuzzy_similarity-based_method_for_failure_detection_and_recovery_time_estimation
8. F. Di Maio, P. Secchi, S. Vantini, E. Zio, Fuzzy C-means clustering of signal functional principal components for post-processing dynamic scenarios of a nuclear power plant digital instrumentation and control system. *IEEE Trans. Reliab.* **60**(2), 415–425 (2011). doi:[10.1109/TR.2011.2134230](https://doi.org/10.1109/TR.2011.2134230)
9. T.M. Cover, P.E. Hart, Nearest neighbor pattern classification. *IEEE Trans. Inf. Theory* **13**(1), 21–27 (1967). doi:[10.1109/TIT.1967.1053964](https://doi.org/10.1109/TIT.1967.1053964)
10. W.R. Nelson, REACTOR: An expert system for diagnosis and treatment of nuclear reactor accidents. *AAAI* 296–301 (1982). <http://www.aaai.org/Papers/AAAI/1982/AAAI82-070.pdf>
11. F. Jamil, M. Abid, I. Haq et al., Fault diagnosis of Pakistan Research Reactor-2 with data-driven techniques. *Ann. Nucl. Energy* **90**, 433–440 (2016). doi:[10.1016/j.anucene.2015.12.023](https://doi.org/10.1016/j.anucene.2015.12.023)
12. B. Papin, G. Beltranda, Computerized monitoring systems: design requirements for a better impact on plant operation. *Used Nucl. Power Plant Accid. Prev. Mitig.* **169** (1989). http://www.iaea.org/inis/collection/NCLCollectionStore/_Public/21/072/21072038.pdf#page=161
13. R. Bhatnagar, D.W. Miller, B.K. Hajek, et al., An integrated operator advisor system for plant monitoring, procedure management, and diagnosis. *Nucl. Technol.* **89**(3), 281–317 (1990). http://www.ans.org/pubs/journals/nt/a_34368
14. K. Haugset, N.T. Førdestrømmen, R.E. Grini, et al., Realisation of the integrated control room concept. *ISACS* (1991). <http://philpapers.org/rec/HAUROT-2>
15. K. Follesø, N.T. Førdestrømmen, K. Haugset, et al., The integrated surveillance and control system ISACS: an advanced control room prototype, in *International Conference on Design and Safety of Advanced Nuclear Power Plants* (Tokyo, 1992). http://www.ans.org/pubs/journals/nt/a_35000
16. T. Endestad, P. Meyer, GOMS Analysis as an Evaluation Tool in Process Control: An Evaluation of the ISACS-1 Prototype and the COPMA System (HWR-349) (1993). http://www.researchgate.net/publication/239280321_Goms_analysis_as_an_evaluation_tool_in_process_control_an_evaluation_of_the_isacs-1_prototype_and_the_copma_system
17. L. Xu, J. Xu, Sensory information fusion-based fault diagnostics for complex electronic systems. *Proc. Inst. Mech. Eng. O: J. Risk Reliab.* **230**(1), 109–119 (2016). doi:[10.1177/1748006X15599125](https://doi.org/10.1177/1748006X15599125)
18. Y. Cui, J. Shi, Z. Wang, An analytical model of electronic fault diagnosis on extension of the dependency theory. *Reliab. Eng. Syst. Saf.* **133**, 192–202 (2015). doi:[10.1016/j.res.2014.09.015](https://doi.org/10.1016/j.res.2014.09.015)

19. D.T. Nguyen, Q.B. Duong, E. Zamai, et al., Fault diagnosis for the complex manufacturing system. *Proc. Inst. Mech. Eng. O: J. Risk Reliab.* 1748006X15623089 (2016). doi:[10.1177/1748006X15623089](https://doi.org/10.1177/1748006X15623089)
20. S. Maza, Diagnosis modelling for dependability assessment of fault-tolerant systems based on stochastic activity networks. *Qual. Reliab. Eng. Int.* **31**(6), 963–976 (2015). doi:[10.1002/qre.1652](https://doi.org/10.1002/qre.1652)
21. J. Xu, K. Sun, L. Xu, Data mining-based intelligent fault diagnostics for integrated system health management to avionics. *Proc. Inst. Mech. Eng. O: J. Risk Reliab.* **229**(1), 3–15 (2015). doi:[10.1177/1748006X14545409](https://doi.org/10.1177/1748006X14545409)
22. J.M.B. de Lázaro, A.P. Moreno, O.L. Santiago et al., Optimizing kernel methods to reduce dimensionality in fault diagnosis of industrial systems. *Comput. Ind. Eng.* **87**, 140–149 (2015). doi:[10.1016/j.cie.2015.05.012](https://doi.org/10.1016/j.cie.2015.05.012)
23. J. Ma, J. Jiang, Semisupervised classification for fault diagnosis in nuclear power plants. *Nucl. Eng. Technol.* **47**(2), 176–186 (2015). doi:[10.1016/j.net.2014.12.005](https://doi.org/10.1016/j.net.2014.12.005)
24. X. Zhang, J. Zhou, J. Guo, Q. Zou et al., Vibrant fault diagnosis for hydroelectric generator units with a new combination of rough sets and support vector machine. *Expert Syst. Appl.* **39**(3), 2621–2628 (2012). doi:[10.1016/j.eswa.2011.08.117](https://doi.org/10.1016/j.eswa.2011.08.117)
25. Z. Geng, Q. Zhu, Rough set-based heuristic hybrid recognizer and its application in fault diagnosis. *Expert Syst. Appl.* **36**(2), 2711–2718 (2009). doi:[10.1016/j.eswa.2008.01.020](https://doi.org/10.1016/j.eswa.2008.01.020)
26. K.Y. Chan, S.H. Ling, T.S. Dillon, H.T. Nguyen, Diagnosis of hypoglycemic episodes using a neural network based rule discovery system. *Expert Syst. Appl.* **38**(8), 9799–9808 (2011). doi:[10.1016/j.eswa.2011.02.020](https://doi.org/10.1016/j.eswa.2011.02.020)
27. J.-D. Wu, C.-K. Huang, Y.-W. Chang, Y.-J. Shiao, Fault diagnosis for internal combustion engines using intake manifold pressure and artificial neural network. *Expert Syst. Appl.* **37**(2), 949–958 (2010). doi:[10.1016/j.eswa.2009.05.082](https://doi.org/10.1016/j.eswa.2009.05.082)
28. J. Palma, J.M. Juarez, M. Campos, R. Marin, Fuzzy theory approach for temporal model-based diagnosis: an application to medical domains. *Artif. Intell. Med.* **38**(2), 197–218 (2006). doi:[10.1016/j.artmed.2006.03.004](https://doi.org/10.1016/j.artmed.2006.03.004)
29. E. Zio, G. Gola, A neuro-fuzzy technique for fault diagnosis and its application to rotating machinery. *Reliab. Eng. Syst. Saf.* **94**(1), 78–88 (2009). doi:[10.1016/j.res.2007.03.040](https://doi.org/10.1016/j.res.2007.03.040)
30. K. Salahshoor, M.S. Khoshro, M. Kordestani, Fault detection and diagnosis of an industrial steam turbine using a distributed configuration of adaptive neuro-fuzzy inference systems. *Simul. Model. Pract. Theory* **19**(5), 1280–1293 (2011). doi:[10.1016/j.simpat.2011.01.005](https://doi.org/10.1016/j.simpat.2011.01.005)
31. Y.-H. Lin, P.-C. Lee, T.-P. Chang, Practical expert diagnosis model based on the grey relational analysis technique. *Expert Syst. Appl.* **36**(2), 1523–1528 (2009). doi:[10.1016/j.eswa.2007.11.046](https://doi.org/10.1016/j.eswa.2007.11.046)
32. C.-H. Lin, C.-H. Wu, P.-Z. Huang, Grey clustering analysis for incipient fault diagnosis in oil-immersed transformers. *Expert Syst. Appl.* **36**(2), 1371–1379 (2009). doi:[10.1016/j.eswa.2007.11.019](https://doi.org/10.1016/j.eswa.2007.11.019)
33. M.P. Cabasino, A. Giua, C. Seatzu, Fault detection for discrete event systems using Petri nets with unobservable transitions. *Automatica* **46**(9), 1531–1539 (2010). doi:[10.1016/j.automatica.2010.06.013](https://doi.org/10.1016/j.automatica.2010.06.013)
34. M.P. Cabasino, A. Giua, M. Poggi, C. Seatzu, Discrete event diagnosis using labeled Petri nets An application to manufacturing systems. *Control Eng. Pract.* **19**(9), 989–1001 (2011). doi:[10.1016/j.conengprac.2010.12.010](https://doi.org/10.1016/j.conengprac.2010.12.010)
35. J. Ding, Y. Cao, E. Mpofu, Z. Shi, A hybrid support vector machine and fuzzy reasoning based fault diagnosis and rescue system for stable glutamate fermentation. *Chem. Eng. Res. Des.* **90**(9), 1197–1207 (2012). doi:[10.1016/j.cherd.2012.01.004](https://doi.org/10.1016/j.cherd.2012.01.004)
36. J. Kurek, S. Osowski, Support vector machine for fault diagnosis of the broken rotor bars of squirrel-cage induction motor. *Neural Comput. Appl.* **19**(4), 557–564 (2009). doi:[10.1007/s00521-009-0316-5](https://doi.org/10.1007/s00521-009-0316-5)
37. J. Pearl, *Causality: Models, Reasoning and Inference*, 2nd edn (Cambridge University Press, Cambridge, 2009). <http://journals.cambridge.org/action/displayFulltext?type=1&fid=153246&jid=ECT&volumeId=19&issueId=04&aid=153245>
38. F.V. Jensen, T.D. Nielsen, *Bayesian Networks and Decision Graphs*, 2nd edn (Springer, Berlin, 2007). http://books.google.com/books?hl=zh-CN&lr=&id=37CAgCykQaAC&oi=fnd&pg=PR5&dq=Bayesian+Networks+and+Decision+Graphs.&ots=f0sioBPP_&sig=i5Kve24fzOgIbnEX0TEZ1ZQ0gJA#v=onepage&q=Bayesian%20Networks%20and%20Decision%20Graphs.&f=false
39. Z. Ghahramani, M.I. Jordan, Factorial hidden Markov models. *Mach. Learn.* **29**(2–3), 245–273 (1997). doi:[10.1023/A:1007425814087](https://doi.org/10.1023/A:1007425814087)
40. H. Ocak, K.A. Loparo, HMM-based fault detection and diagnosis scheme for rolling element bearings. *J. Vib. Acoust.* **127**(4), 299–306 (2005). doi:[10.1115/1.1924636](https://doi.org/10.1115/1.1924636)
41. S. Ntalampiras, Y. Soudopionis, G. Giannopoulos, A fault diagnosis system for interdependent critical infrastructures based on HMMs. *Reliab. Eng. Syst. Saf.* **138**, 73–81 (2015). doi:[10.1016/j.res.2015.01.024](https://doi.org/10.1016/j.res.2015.01.024)
42. N.L. Zhang, Hierarchical latent class models for cluster analysis. *J. Mach. Learn. Res.* **5**, 697–723 (2004). <http://www.jmlr.org/papers/volume5/zhang04a/zhang04a.pdf>
43. D. Li, D. Cheung, X. Shi et al., Uncertainty reasoning based on cloud models in controllers. *Comput. Math Appl.* **35**(3), 99–123 (1998). doi:[10.1016/S0898-1221\(97\)00282-4](https://doi.org/10.1016/S0898-1221(97)00282-4)
44. Q. Zhang, Dynamic uncertain causality graph for knowledge representation and reasoning: discrete DAG cases. *J. Comput. Sci. Technol.* **27**(1), 1–23 (2012). doi:[10.1007/s11390-012-1202-7](https://doi.org/10.1007/s11390-012-1202-7)
45. Q. Zhang, Dynamic uncertain causality graph for knowledge representation and probabilistic reasoning: directed cyclic graph and joint probability distribution. *IEEE Trans. Neural Netw. Learn. Syst.* (2015). doi:[10.1109/TNNLS.2013.2279320](https://doi.org/10.1109/TNNLS.2013.2279320)
46. Q. Zhang, C. Dong, Y. Cui et al., Dynamic uncertain causality graph for knowledge representation and probabilistic reasoning: statistics base, matrix, and application. *IEEE Trans. Neural Netw. Learn. Syst.* **25**(4), 645–663 (2014). doi:[10.1109/TNNLS.2013.2279320](https://doi.org/10.1109/TNNLS.2013.2279320)
47. Q. Zhang, Dynamic uncertain causality graph for knowledge representation and reasoning: continuous variable, uncertain evidence, and failure forecast. *IEEE Trans. Syst. Man Cybern. Syst.* (2015). doi:[10.1109/TSMC.2015.2392711](https://doi.org/10.1109/TSMC.2015.2392711)
48. Q. Zhang, S. Geng, Dynamic uncertain causality graph applied to dynamic fault diagnoses of large and complex systems. *IEEE Trans. Reliab.* (2015). doi:[10.1109/TR.2015.2416332](https://doi.org/10.1109/TR.2015.2416332)
49. C. Dong, Y. Wang, Q. Zhang et al., The methodology of dynamic uncertain causality graph for intelligent diagnosis of vertigo. *Comput. Methods Programs Biomed.* **113**(1), 162–174 (2014). doi:[10.1016/j.cmpb.2013.10.002](https://doi.org/10.1016/j.cmpb.2013.10.002)
50. Y. Zhao, Q. Zhang, H.C. Deng, Application of DUCG in fault diagnosis of nuclear power plant secondary loop. *Atomic Energy Sci. Technol.* **48**(1), 496–501 (2014). doi:[10.7538/yzk.2014.48.S0.0496](https://doi.org/10.7538/yzk.2014.48.S0.0496) (in Chinese)
51. Y. Zhao, C.L. Dong, Q. Zhang, Fault diagnostics using DUCG in complex systems. *J. Tsinghua Univ. (Sci. Technol.)* **56**, 530–537 (2016). doi:[10.16511/j.cnki.qhdxxb.2016.25.012](https://doi.org/10.16511/j.cnki.qhdxxb.2016.25.012) (in Chinese)